

## 2. ACCELERATOR AUGMENTATION PROGRAM

### 2.1 LINAC

S.Ghosh, A.Rai, P.Patra, G.K.Chowdhury, B.K.Sahu, A.Pandey, D.S.Mathuria, J.Karmakar, S.S.K.Sonti, K.K.Mistry, R.N.Dutt, A.Sarkar, R.Joshi, R. Ahuja, R. Kumar, S.K.Suman. J.Chacko, A.Chowdhury, S.Kar, S.Babu, M.Kumar, J.Antony, J.Zacharias, P.N.Prakash, T.S.Datta, D.Kanjilal and A.Roy

#### 2.1.1 Operation of all five cryostats of Superconducting Linac and delivery of energised beam for scheduled experiments



Fig. 1. The first picture shows the three accelerating module of the Superconducting Linear accelerator of IUAC. The second picture shows the last linac accelerating module being installed with six resonators.

The complete linear accelerator (Linac) system of Inter University Accelerator Centre was designed to have five cryostats, the first one acting as superbuncher with a single quarter wave resonator (QWR), the next three linac cryomodules house eight QWRs each, and the last one has two QWRs used as rebuncher.

In the year 2012, the last linac accelerating module was installed with six QWR (as shown in the second picture of figure 1) and it was successfully tested with liquid helium. From November 2012, all the three accelerating modules along with the superbuncher and rebuncher were operational and different ion species from Pelletron accelerator were further accelerated by linac and were delivered for scheduled experiments in the beam line of HYbrid Recoil mass Analyser (HYRA). The list of the ion beam accelerated through linac is given in table-1. During this operation, no major problem was encountered and the facility was operational for about three months to complete all the scheduled experiments.

**Table:1. Maximum energy gain from different ion species from the three accelerating linac modules**

Beam species	Energy from pelletron (MeV)	Time width @ Linac Entrance	Energy gain from LINAC (MeV)	Total Energy (MeV)	Experimental Area
$^{48}\text{Ti}^{14+}$	162	~204 ps	108	270	HYRA
	162	~185 ps	95	257	HYRA
$^{28}\text{Si}^{12+}$	112	~132 ps	84	196	HYRA
$^{28}\text{Si}^{11+}$	124	~143ps	65	187	HYRA
$^{28}\text{Si}^{8+}$	110	~225ps	50	160	HYRA
$^{30}\text{Si}^{2+}$	100	~260ps	80	180	HYRA

### 2.1.2 Activities related to improvement of the performance of the resonator and automation of linac operation

To increase the performance of the accelerating fields and hence the energy gain of the ion beam from the linac, several steps and modifications are implemented and they are listed in the following:

- a) A warm water (~ 75 oC) ultrasonic rinsing facility is being used routinely as the final step of the surface preparation process of the niobium quarter wave resonator (QWR) prior to load them in the cryostat. Many laboratories have found that warm water ultrasonic rinsing reduces the field emission and helps to improve the accelerating fields of the niobium resonators.
- b) A separate tuning mechanism based on the Piezo actuator was designed and tested on a few resonators in the past. During the last cold test, in linac-3, mechanical tuning by Piezo actuator was implemented in four out of six resonators and their performance was excellent. A number of advantages of the piezo tuning mechanism are observed over the existing gas tuning mechanism as mentioned below,
  - Phase lock mechanism of the resonator has become easier
  - The stability of the phase lock has been improved
  - The requirement of the average power during phase locking is reduced substantially.

All the gas based tuning mechanism installed on the resonators of linac-2 and 3 are planned to be replaced by piezo actuator based tuning mechanism.

- c) It is well known that microphonics coupled to the resonator can cause a frequency jitter in the resonance frequency of a superconducting resonator and extra RF power may be required to phase lock it. To reduce RF power requirement, a vibration damping mechanism with SS-balls of a particular diameter had been incorporated in the past on the first group of resonators built in USA in collaboration with Argonne National Lab. However, the same diameters of SS-balls are not proven to be optimum for the resonators made at IUAC. So the experiments related to vibration damping mechanism using SS-balls had been repeated with the resonators built indigenously at IUAC. During this investigation, SS-balls (diameter from 6 mm to 12 mm) with bigger diameter (what was not tried before) and a mixture of SS-balls with different diameters were tried out at room temperature and the results were encouraging. The optimum number and diameter of the SS-balls yielded the best results during the experiments carried out at room temperature were inserted in all the resonators of linac-2 and 3. However, the optimum number and diameter of SS balls found for the best vibrational damping at room temperature has to be validated by more tests of the resonators kept at liquid helium temperature.
- d) Since last few years, a mechanism to phase lock a superconducting linac resonator from remote location (linac control room) has been used for routine operation. Recently, up-gradation of the existing mechanism has been successfully implemented. In this mechanism, when a superconducting resonator is going out of its frequency and phase lock, electronically the resonance frequency of the resonator is sensed and a corresponding voltage signal is generated to do the necessary correction of the resonance frequency of the resonator to bring back its frequency close to the master oscillator. When the frequency of the resonator becomes very close to master oscillator, then the phase lock circuit of the resonator will be put on electronically. During last linac operation, this 'Auto Locking' mechanism has been successfully tested on a number of resonators.
- e) A capacitive pick up loop has been installed at the exit of linac beam line and has been tested successfully. After the successful test of this device, it was decided that couple of capacitive pick up loop will be installed in the linac beam line to measure the beam energy while tuning the linac. Since it is a passive device, so beam doesn't need to be stopped on gold foil to measure the energy by surface barrier detector. Installing another capacitive pick up loop is also being planned after the superbuncher to measure the time width of the beam bunch prior to its injection in to linac resonators.

- f) A separate cooling arrangement for the power coupler of the resonator is designed, fabricated and installed in all the drive couplers of the resonators of the last linac cryostat (linac-3). The same cooling arrangements will be installed in all the resonators of linac-1 and 2 in the next opening of the cryostat. This new modification adds extra protection of the coupler and the power cable from overheating and helps to increase the accelerating field of the resonators.

### 2.1.3 Superconducting Niobium Resonators

P.N.Prakash, S.S.K.Sonti, K.K.Mistri, A.Rai, J.Sacharias, D.Kanjilal & A.Roy

Fabrication of the two SSR1 Single Spoke Resonators for Project-X of Fermi National Accelerator Laboratory (FNAL) is nearing completion. A 5-cell 1.3 GHz TESLA-type Cavity has been successfully developed under a joint collaboration between IUAC and Raja Ramanna Centre for Advanced Technology (RRCAT), Indore. Development of a 650 MHz,  $\beta=0.9$  single cell cavity has also started under this collaboration. In addition, there are plans to develop a 650 MHz,  $\beta=0.6$  single cell cavity in collaboration with Variable Energy Cyclotron Centre (VECC), Kolkata.

#### 2.1.3.1 Single Spoke Resonators

Fabrication of the two Single Spoke Resonators ( $\beta=0.22$ ,  $f=325$  MHz) for Project-X of Fermi National Accelerator Laboratory (FNAL), USA, has advanced sufficiently. Two, out of the three, major assemblies, namely the End Walls and the Outer Shells, have been completed and work is progressing for completing the third assembly - that is the Spoke. In figure 1, the RF surface of an electropolished End Wall assembly is shown. In figure 2, an isometric view of the Spoke assembly is shown. The Spoke to Shell Collar, which provides the transition from the Spoke to the Outer Shell, was first developed. The assembling of the bare-Spoke with its Shell Collars required extensive fixturing for proper orientation and alignment. In figure 3a, this setup is shown. Separately fixtures for electron beam welding were designed and fabricated. In figure 3b, the electron beam welding setup for attaching the Spoke to the Shell Collar, is shown.



Fig. 1. RF surface of an electropolished End Wall for the Single Spoke Resonator -SSR1.

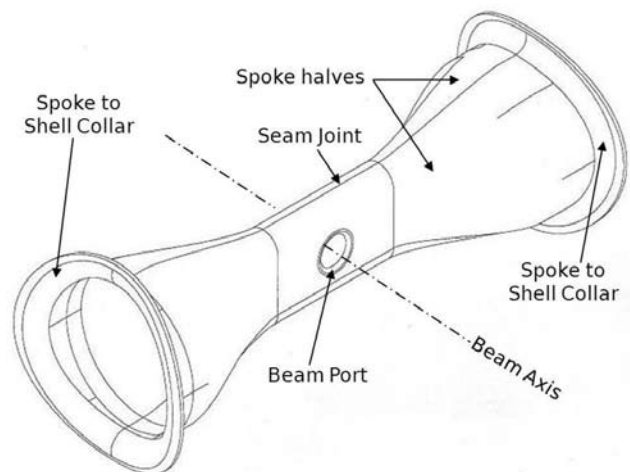


Fig. 2. Isometric view of the Spoke assembly showing its various components.

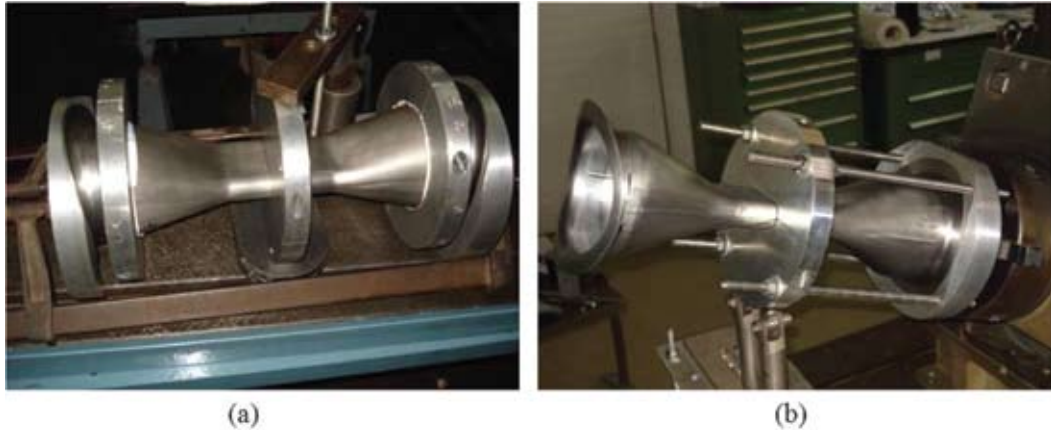


Fig. 3. (a) Setup for assembling the Spoke and Shell Collars to ensure proper clocking and alignment of the components, (b) setup showing the electron beam welding of the Shell Collar to the Spoke.

The Spoke assemblies are now getting ready for electropolishing before they are attached to the Shell. This will be followed by frequency tuning of the resonator and finally electron beam welding of the End Walls to the Shell.

#### 2.1.3.2 TESLA-type 5-Cell, 1.3 GHz Cavity

Under the Indian Institutions and Fermi Lab Collaboration (IIFC), Raja Ramanna Centre for Advanced Technology (RRCAT), Indore and IUAC had successfully developed 1.3 GHz TESLA-type single cell niobium cavities. Before embarking on the more difficult and risky 1.3 GHz 9-cell cavity, it was decided to first jointly develop a 5-cell cavity with simple end tubes. This decision was also dictated by the available travel length and chamber size in the IUAC electron beam welding machine. In figure 4, the two halves of the 5-cell cavity are shown. In figure 5, the completed 5-cell cavity is shown. This is the first time that a multi-cell niobium cavity has been successfully built in India. The cavity would be sent to FNAL for testing at 2 K.



Fig. 4. The two halves of the 5-cell TESLA-type Cavity.



Fig. 5. The first 5-cell TESLA-type Cavity built in India.

### 2.1.3.3 650 MHz, $\beta=0.9$ Cavity

The accelerator design for Project-X at FNAL was changed some time ago by incorporating 650 MHz cavities in place of 1.3 GHz TESLA-type cavities. RRCAT and IUAC have therefore decided to develop 650 MHz,  $\beta=0.9$  cavities. As with the 1.3 GHz TESLA-type cavities, the development of the 650 MHz cavities is also being taken up in stages. In the first stage single cell cavities would be developed. After successfully fabricating and testing them, 650 MHz multi-cell cavities would be built.

Development of a 650 MHz,  $\beta=0.9$  single cell cavity has been initiated. The forming and machining of the cavity components is being done at RRCAT. The electron beam welding is performed at IUAC. In figure 6a, an end tube setup for electron beam welding of the seam joint, is shown. In figure 6b, the tube to Nb-Ti flange welding setup is shown.



Fig. 6. (a) Electron beam welding setup for the seam welding of the end tube, (b) setup showing the electron beam welding of the tube to Nb-Ti flange.

The half cells for fabricating the first cavity have been formed and trials for parameter development of the crucial equator joint will begin soon. We plan to complete the fabrication of the cavity in the first half of the present calendar year.

## 2.2 HCI

### 2.2.1 High Temperature Superconducting ECRIS -PKDELIS and Low Energy Beam Transport (LEBT)

**G.Rodrigues, Y.Mathur, P.S.Lakshmy, R.Ahuja, K.Mal, R.N.Dutt, N. Aggarwal, A.Mandal, D.Kanjilal & A.Roy**

#### A. 18 GHz High Temperature Superconducting ECR ion source, PKDELIS

In the last academic year, the performance of both the cryo-coolers were not satisfactory and in addition to the large room temperature fluctuations (from 18°C to 26°C), the injection cryo-cooler used to trip very often due to high room temperature. During the course of running of the cryo-coolers, it was also observed that the extraction cryo-cooler body was turning very hot inspite of the main exhaust fan in working condition. This was not the case with the injection cryo-cooler body. Due to the high temperature and continuous operation, a leak developed in the system and due to this leak, the helium pressure was slowly falling over a period of few months. The extraction cryo-cooler was shut down with a lower helium pressure and a systematic leak test was performed with a He sniffer detector. Unfortunately, exact pin-pointing of the leak could not be carried out. A quick soap bubble test was performed over all the joints and finally the

leak was located on a solenoid valve (see figure 1). Most likely the o-ring of the solenoid valve had gone bad. Considering the total amount of time, the cryo-cooler had operated and due to the non-availability of this kind of solenoid valve, it was decided to replace the existing cryo-cooler with a new one. Various works were carried out to get the interlocks working with the new cryo-cooler, including a new type of exhaust to match with new exhaust fan design in the new cryo-cooler. The system was finally integrated with the cold head at the extraction side. The system has been found to be working satisfactorily.



Fig. 1. Location of the solenoid valve and leak location in the extraction cryo-cooler using soap solution.



Fig. 2. View of the new extraction cryo-cooler installed

The tripping problem of the injection cooler was looked into after replacing the extraction cooler. It was observed that the heat exchanger was severely clogged with dust and needed maintenance. Additionally, since the system had completed more than 40,000 hours of operation similar to the extraction cryo-cooler, it was decided to replace the existing one with a new cryo-cooler. Similar works had to be carried out to get the interlocks in working condition, including a new type of exhaust to match with new exhaust fan design in the new cryo-cooler. The system was finally integrated with the cold head at the injection side. The system has been found to be working satisfactorily.

With both the cryo-coolers operating, the room temperature variations are still not permitting for smooth operation of the system. This is being looked into. It is expected that as soon as the room temperature problem is fixed, the system can be made to run in a smoother way.

## B. Electronics and related maintenance Activities

- (i) A 250W 8GHz to 18GHz Traveling Wave Tube (TWT) amplifier of Amplifier research, U.S.A. make (model: 200T8G18) for PKDELIS ECR ion source lab had gone bad while it was being temporarily used in the Low energy ion beam facility (LEIFF). On checking it was then found that its power factor correction (PFC) module had gone bad. Its interface card was also not functioning properly. On inspecting and checking the PFC module in detail we found that two MOSFETs 5010BLV which were used to convert the line voltage to DC and as well as improve the power factor had gone bad. One thermistor at line input and one 560 uF 400 V capacitors at the DC output of this module were also faulty. The power factor correction (PFC) module and the interface board have been repaired successfully (which could not be repaired by the authorized service agent of

M/s Amplifier Research) by replacing above mentioned faulty components in PFC module and by properly inserting the analog to digital (ADC) ICs in interface card. This amplifier was then tested for full power on dummy load. This maintenance has saved more than US\$ 5000 of IUAC and as well as creating stock of spare modules of PFC and interface boards.

- (ii) 30kV, 20mA high voltage DC power supply (M/s Glassman make) being used for the beam extraction in the 2.45GHz ECR ion source had gone bad. On detailed checking we found that capacitor C33, 47uF/35V, in its low voltage dc power supply filter section had gone faulty (short). We repaired it by replacing the faulty capacitor and tested it for full rated voltage on dummy load for than 8 hours.
- (iii) A two channel gas valve controller has been developed for ECR ion source applications. Previously similar instrument was being imported. This indigenously developed controller can be used to remotely control the two needle gas valves independently to vary the gas pressure and hence helps in tuning of the beams remotely. Specification wise this controller is at par with the imported controller but in cooling aspects it is better, considering typical indian temperature and climatic conditions.
- (iv) The 50 KVA UPS which is presently being utilized for the 18 GHz high temperature superconducting ECR ion source, PKDELIS and LEBT had undergone major maintenance in this year. It was not giving any output and hence no back-up during power failures. It got repaired through the authorized service agents under AMC with them. Two rectifier board and controller card were replaced. Later we also replaced all the 30 batteries under preventive maintenance as they were more than 5 years old. The UPS is now functioning properly.

#### **C. Control system upgrade and connectivity to PCLI**

The control system for the 18 GHz high temperature superconducting ECR ion source and LEBT has been upgraded and connectivity to PCLI established. The central control system of IUAC runs a high level protocol using an Ethernet TCP/IP based central control scheme. A distributed control topology is used to enable control from the control room of IUAC. Several enhanced control functions are available in the local mode. Local control also supports enhanced graphics and GUI based control functionality. For the smooth functioning of the control system at the server location (close to the ECR source in beam hall III), only few important source control parameters will be available at the client in the control room, the remaining source control parameters will be at the server and all parameters will be available as readback at the client location. Assuming that the ion source and LEBT are first tuned locally at the server location, transfer of control will be made available at the client, henceforth. The source and LEBT in general will not be available for complete tuning of the beam at the client location, unless control is provided by the server.

#### **D. New optics on the 100 kV high voltage platform**

The complete ion optics on the 100 kV high voltage platform has been re-done to take into account the asymmetrical 3D beam shape from the ion source and to also consider incorporation of a focusing element before the analyzing magnet to correct for double focusing at the image plane. Due to the asymmetrical beam shape from the ion source, corrections for the higher order aberrations are necessary for achieving good mass resolution for the heavier ions.

#### **E. 2.45 GHz ECR Source and LEBT activities**

##### **(i) Testing of 2.45 GHz ECR source**

The 2.45GHz ECRIS which is installed on the existing deck of Room No. 117 has been tested with H<sup>+</sup> and N<sup>+</sup> beams. The existing beam line has been modified due to leak in the accelerating column and a new

beam line has been installed with an additional electrostatic quadrupole triplet. Fig. 3 shows a schematic view of the modified beam line and Fig. 4 shows a typical charge state distribution spectrum obtained from  $N_2$  plasma. A few ion implantation experiments also have been carried out using  $N^+$  beam on Si and GaAs substrates at 20 keV to study phase formation on the surface of the samples. Source has been tested with different axial magnet configuration and found that beam intensity falls drastically as the injection side magnet ring moves away from the microwave launching position. This is consistent with the x-ray bremsstrahlung, measured from the source plasma at a distance of 3.65 m through  $0^\circ$  view port of the analyzer magnet, in which the bremsstrahlung intensity falls as the injection magnet ring moves away from the microwave window.

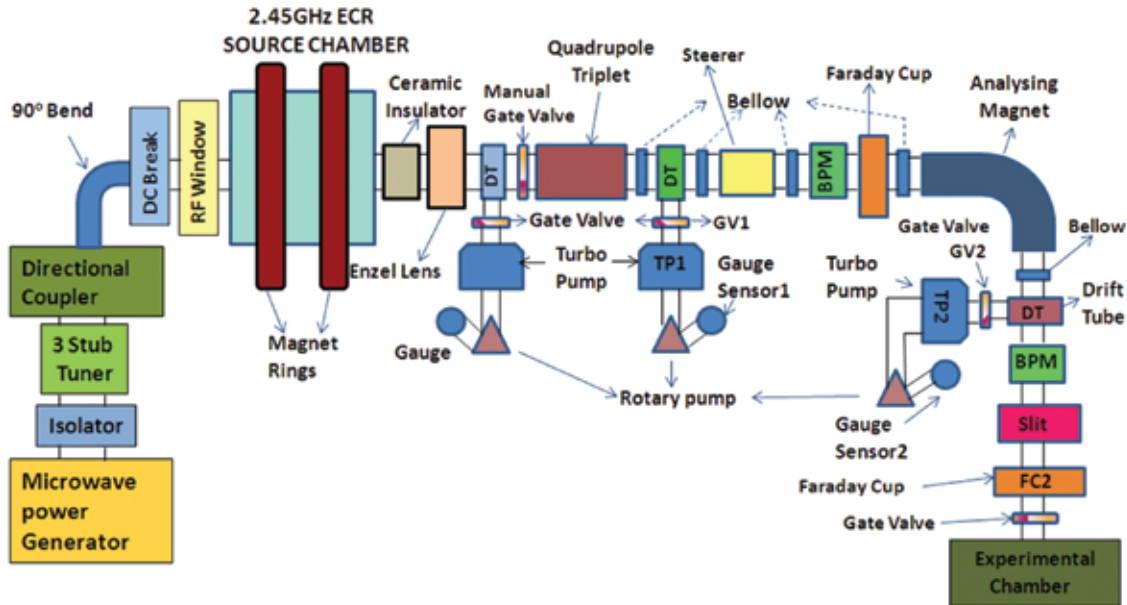


Fig.3. Schematic view of modified beam line in room no.117

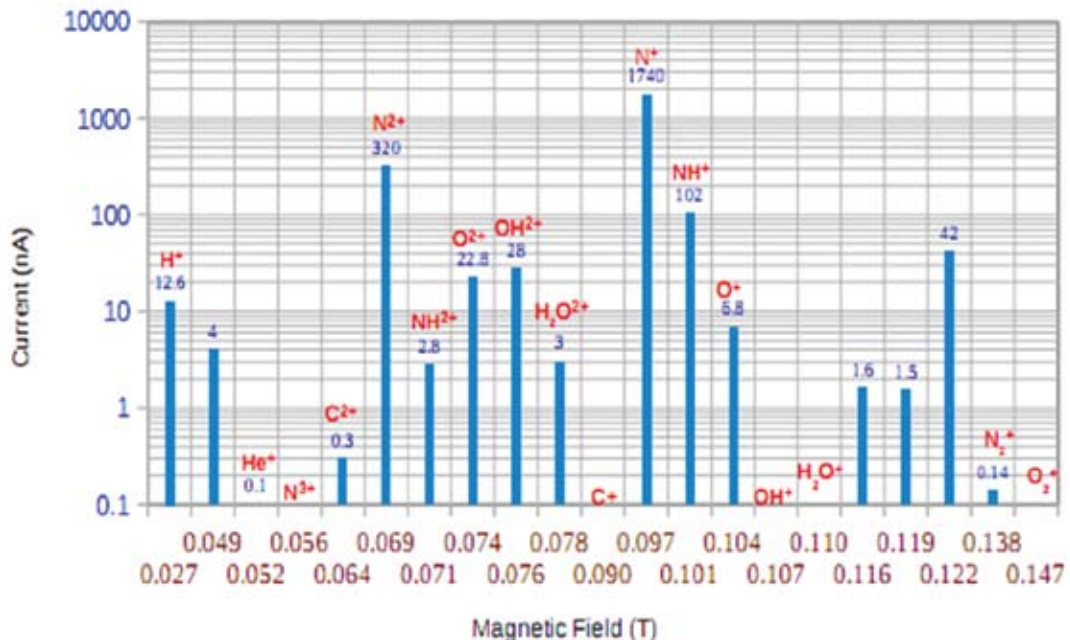


Fig.4. CSD from  $N_2$  plasma at 20 W RF power



As per the design of the plasma chamber, magnet ring cannot be taken closer than 3.9 cm towards the microwave window. During source operation, requirement of a modified compact extraction system with multi electrodes and water cooling for the plasma chamber have been realized.

**(ii) Design, fabrication and assembly of a new water cooled plasma chamber**

Based on the test results of the air cooled source, the design of a new water cooled plasma chamber has been finalized. The plasma chamber is a double walled stainless steel cylindrical cavity having an inner diameter of 90 mm and length of 101 mm. The dimensions of the resonant cavity have been chosen to excite the  $TE_{111}$  dominant mode at 2.45 GHz. The total length of the chamber has been kept 135mm in order to accommodate the magnet structure. The injection side flange of the chamber has been extended towards the waveguide so as to match the injection magnet ring with the microwave launching position.

The water cooling arrangement consists of cooling channels all around the chamber wall and a rib arrangement inside the double walled chamber which separates warm and cold water. Two orthogonal ports have been provided for carrying out plasma diagnostic studies. Plasma chamber has been fabricated and assembled using new set of magnet rings whose magnetic field distribution has been mapped. The left side of Fig. 5 shows the assembled view of the modified source and the source assembly on a movable chariot is shown in the right side of Fig. 5. A movable high voltage platform also has been incorporated together with the source in order to facilitate ease of maintenance activities.

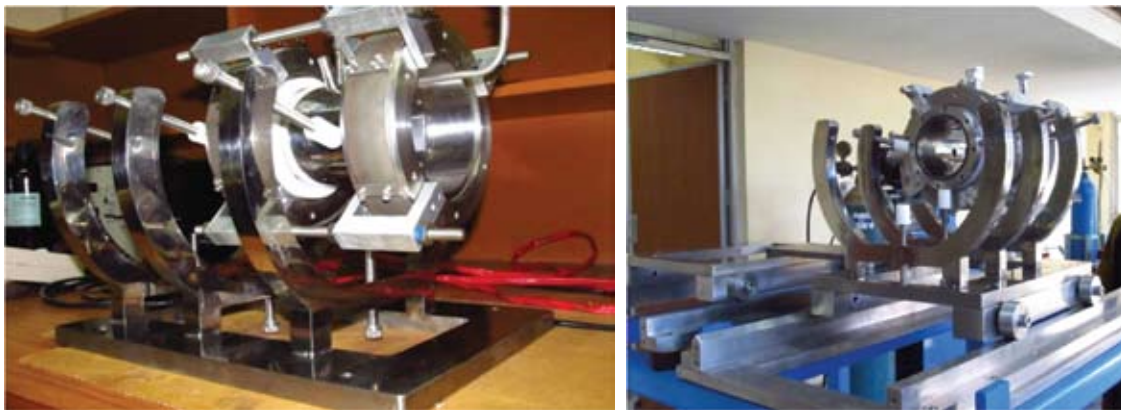


Fig. 5. (Left) View of new source assembly (Right) new source assembly on movable chariot with HV platform

**(iii) Design of a ridge waveguide for 2.45 GHz ECR ion source**

A ridge waveguide has been designed to maximize the electric field on the axis of the plasma chamber (operating in the  $TE_{111}$  mode) (Fig. 6). Due to the particular design constraints, and ease of fabrication, the total length of the waveguide was split in two parts with provision for water cooling in both sections. By simulating an inlet water temperature of 15°C with 4 bar pressure, the outlet temperature rise was only 1°C for cooling the waveguide with 1 kW of RF power. From Fig. 7, it can be seen that the joint between the waveguides shows a maximum average temperature of 49°C, clearly showing that the joint has less cooling capacity as compared to the location of the cooling channels. The ridged waveguide is presently under fabrication.

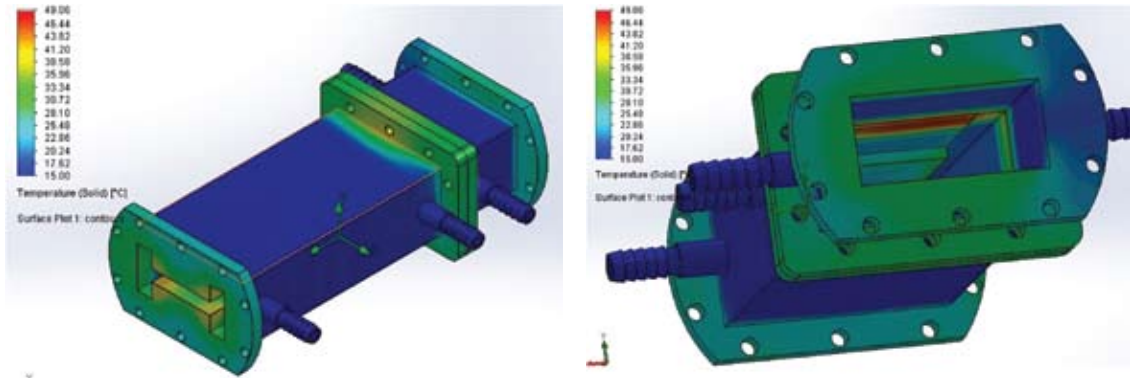


Fig. 7. (Left) Temperature distribution in the waveguide (Right) Maximum temperature at the joint of the waveguides

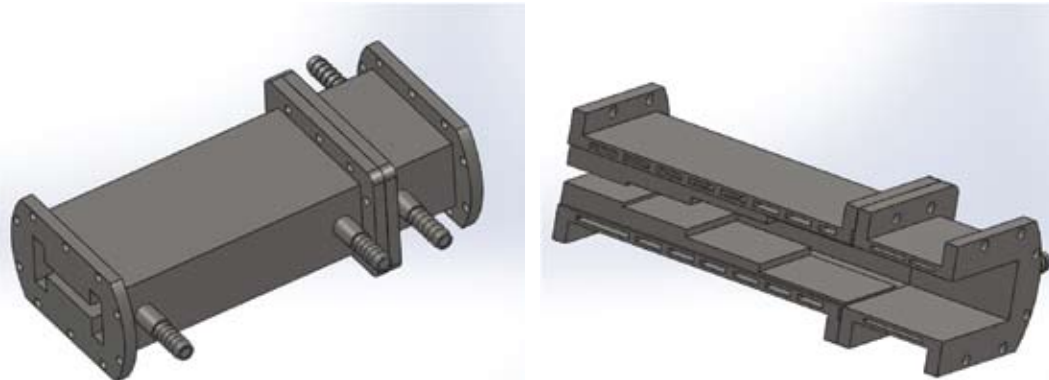


Fig. 6. (Left) View of complete ridge waveguide (Right) View of the inner part of the waveguide showing the cooling channels

#### F. The extraction of intense ion beams from a high field ECR into a RFQ channel

The ion current from high intensity ECR sources for highly charged ions becomes limited during extraction by the high space charge. This makes classical extraction systems for the transport and subsequent matching to a RFQ accelerator less efficient and practically very difficult. The DPI (direct plasma injection) developed for a laser ion source avoids these problems and uses the combined focusing of the gap between the ion source and the RFQ vanes (or rods) and the rf-focusing of the RFQ penetrating into this gap. For high performing ECR sources, using sc solenoids, in addition to the DPI scheme, also the magnetic stray field of the source may be used to provide focusing against the beam space charge. We have designed and optimized a combined extraction/matching system (Fig. 8) for a high performing ECR ion source into a RFQ channel, allowing to form a beam of about 20 mA highly charged  $^{238}\text{U}^{40+}$  at modest ion source voltages of 60 kV. In order to proceed, we have used the feature of IGUN to take into account the rf-focusing of a RFQ channel (without modulation), the electrostatic field between ion source extraction and the RFQ vanes, the magnetic stray field of the ECR superconducting solenoid, and the defocusing space charge of an ion beam. We can show, that the magnetic stray field (dashed line in green colour, the field values are shown on the vertical axis on the right,) becomes essential for this design and that even small variations of 10% are not acceptable. The normalised rf focussing force parameter is plotted with a red dashed line and corresponding values are shown on the vertical axis in the centre of the plot. This work is still in progress and is in collaboration with Goethe University, Frankfurt, and Scientific Software Services, Germany [1]

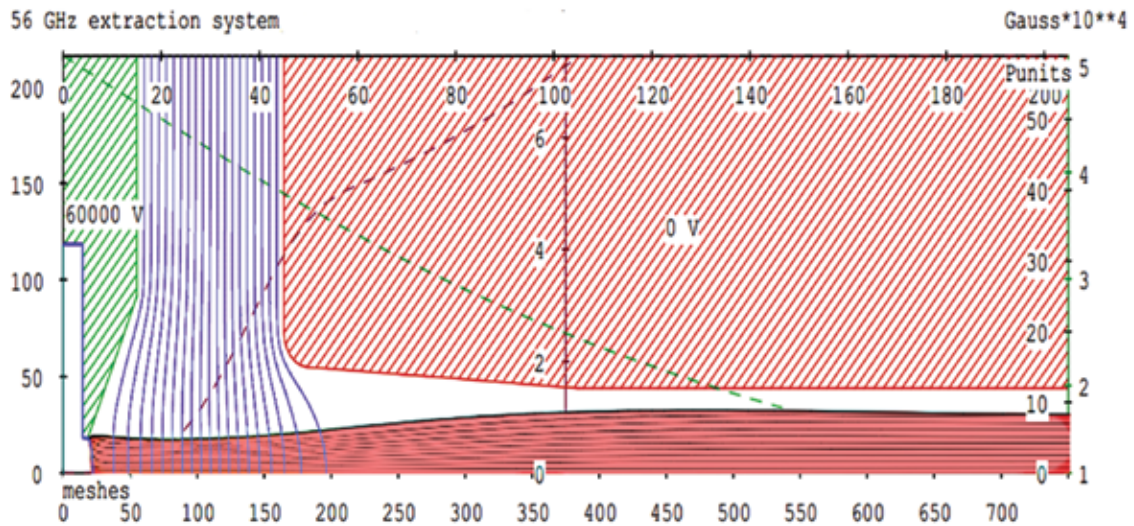


Fig. 8. Combined extraction/matching system for a high performance ECR ion source into a RFQ channel

## References

- [1] R.Becker, private communication

### 2.2.2 Design of the 100 kV high voltage platform for the High Current Injector Programme

G.Rodrigues, Y.Mathur, P.S.Lakshmy, R.Ahuja, A. Kothari, P. Barua, A.Mandal, D.Kanjilal & A.Roy

The beam optics design of the high current injector (HCI) necessitates a stringent requirement on the space available in beam hall III especially on the layout of the main components of the high current injector viz., ECR on a 100 kV high voltage platform, RFQ and DTL. Therefore, the total area of the 100 kV high voltage platform was optimized carefully keeping in mind the space required on the platform for various associated systems related to the ECR ion source, focusing elements and for easy maintenance purposes. The total area of the platform was frozen to 4.5 m x 5.0 m keeping the smaller dimension to fit into the total length of the beam hall (Fig. 9). Considering the fixed injection energy of the RFQ of 8 keV/u, and keeping the maximum available voltage on the source to 20 kV, it was estimated the remaining part of the beam energy would be supplied by the high voltage platform. There were some considerations also to perform a few stand-alone experiments in atomic/molecular physics and materials science using the maximum available energy from high voltage platform. Therefore, the maximum voltage of the high voltage platform was tentatively kept at 100 kV keeping all these considerations in mind. Due to the large number of components to be placed on a wide area of the platform, load bearing capacities of the high voltage insulators including the total number of insulators required were looked into carefully. A typical 200 kV high voltage insulator from LAPP, USA having compression strength of 66.7 kN was chosen which fitted well for the application. Considering the close proximity of the AC ducting in beam hall III at the location of the high voltage platform, the total height of the platform was chosen to be 2.8 m from ground. Due to the available height of the 200 kV high voltage insulators, the beam height of the ECR ion source with respect to the high voltage platform was kept at 1.0 m with considerations coming from the ease of maintenance of the source and the existing height of the hole already drilled through the wall of beam hall III for beam to enter to beam hall I. The model calculations depicting the static displacement and static nodal stress for the base plate and frame support have been simulated using ANSYS. These are shown in Fig. 10 & 11. The fabrication of the 100 kV high voltage platform was given to Vacuum Techniques, Bangalore who were found competent and capable for this kind of work.

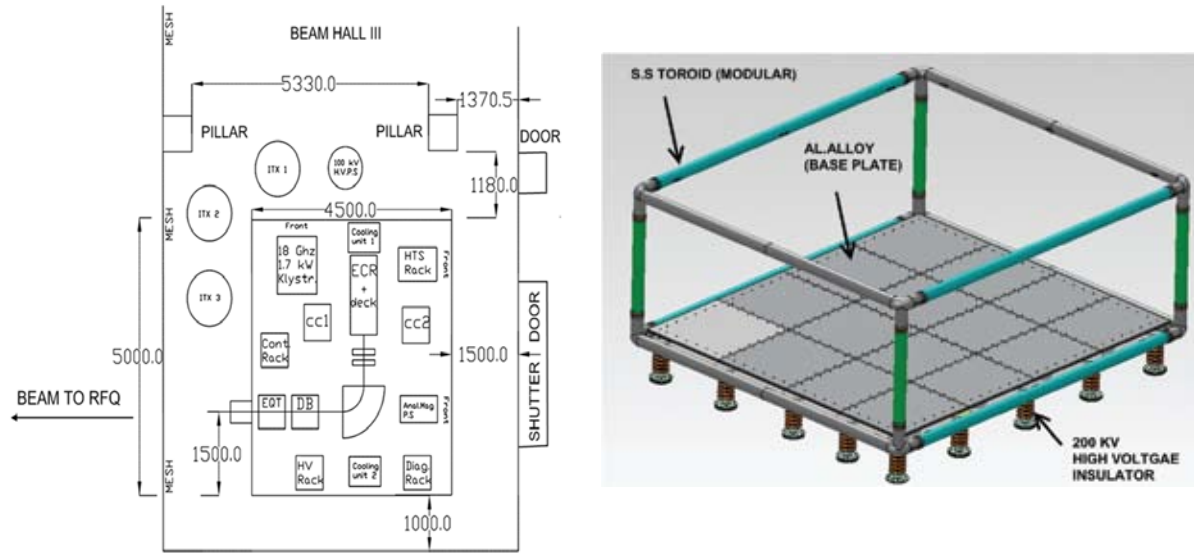


Fig. 9.(Left)View of the layout of ion source and related components on 100 kV high voltage platform, isolation transformers (ITX1,ITX2,ITX3) and 100 kV high voltage power supply positioned in the beam hall III (all dimensions in mm) ; (Right) View of the designed 100 kV high voltage platform

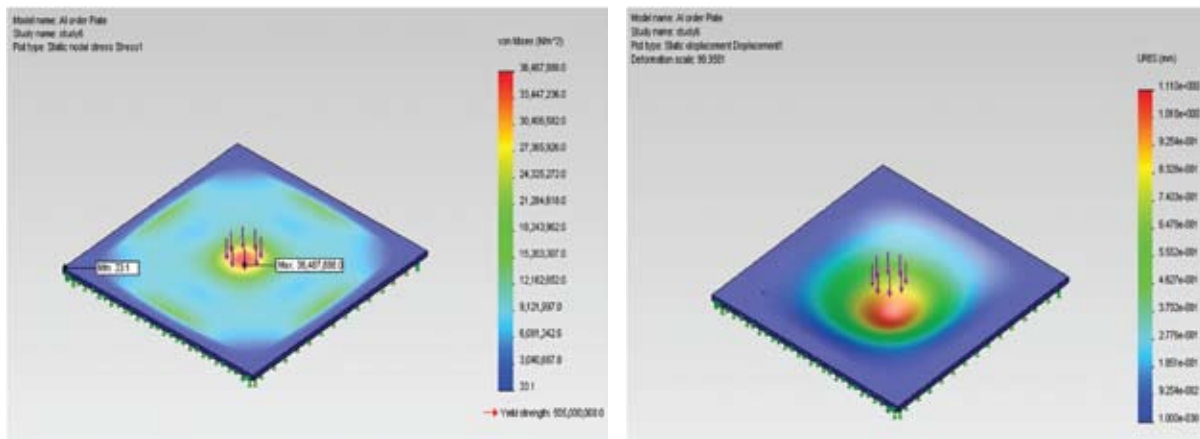


Fig. 10. (Left) Static nodal stress model for the base plate (Right) Static displacement model for the base plate

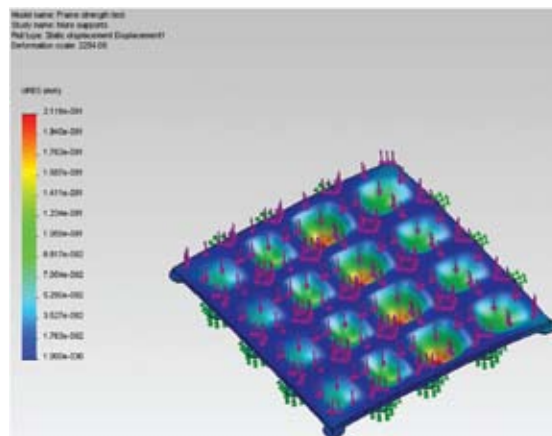


Fig. 11. Static displacement model for the frame support

### 2.2.3 Radio Frequency Quadrupole Accelerator

Rajeev Ahuja, Ashok Kothari, Sugam Kumar ,C. P. Safvan & D. Kanjilal

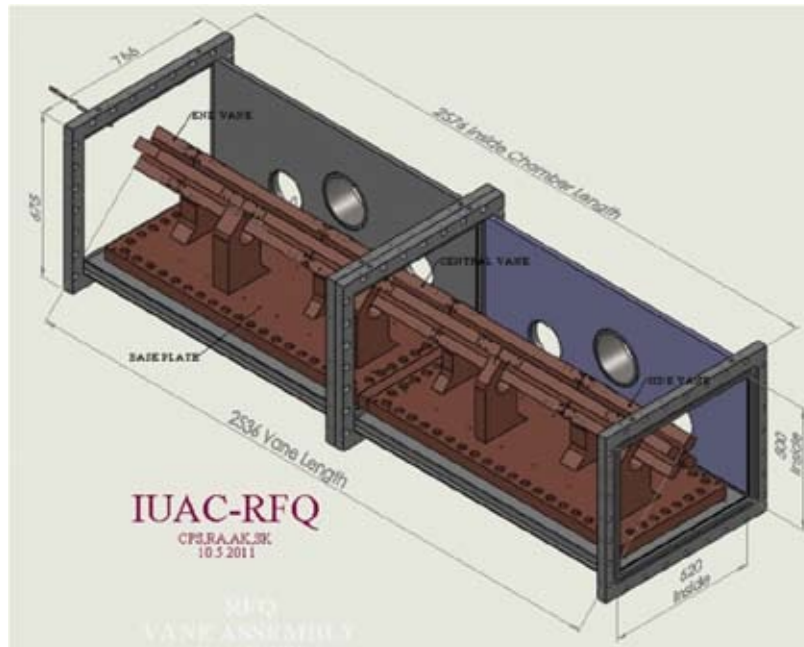


Fig.1. Solid Works Model of the Final RFQ

After the successful completion of the prototype RFQ, we have completed the designing of the final RFQ and the fabrication work has been started. Vacuum chambers have been fabricated, tested & copper plated. Inner components are being fabricated.

The following are the basic requirements/characteristics of the final RFQ

- Total Length of Vanes : 2536mm
- Aperture : 12 mm
- Inner Dimensions of Chamber: 620(W) x500(H) x2576(L) mm etc.

#### Design :

The final RFQ will have two copper plated vacuum chambers with water cooling provision all around. Both the chambers will be assembled together to make one single cavity. There will be two base plates, made of solid copper, which will hold eight vane supports. These vane supports will hold the vanes which are being fabricated in twenty pieces. Water will flow into vanes through vane posts. The chambers will be kept on a stand which will have the provision for alignment in all the three axis. All design and drawing work has been done using solid works. The bottom plate of both the chamber has been machined perpendicular to the side flange to an accuracy of  $0.1^\circ$ , so that both the chambers are straight after assembly. Like prototype RFQ, the bottom plates are the back bone of the chambers. Bottom plates will hold the copper base plates. The base plates will be aligned with the help of portable co-ordinate measuring machine (CMM) as was done in the prototype RFQ. The static, buckling & pressure design analysis was also done by using solid works.

#### Present Status :

Vacuum Chambers are ready. Inner components are being fabricated at Indo German Tool Room, Ahamdabad. Sample modulated vane has been successfully fabricated.

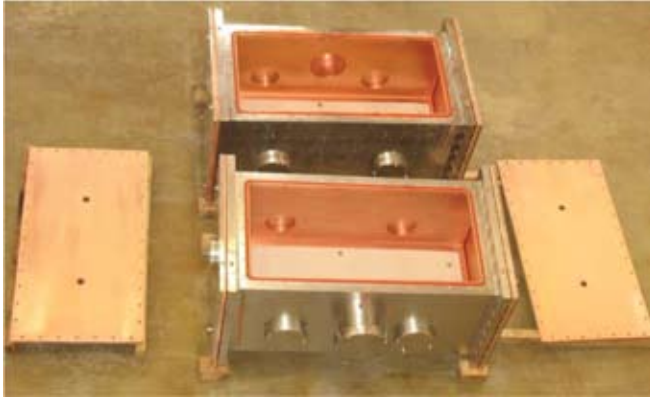


Fig.2. Both the vacuum chambers being leak checked in assembled conditioned at IUAC



Fig.3. Copper Plated Vacuum Chambers at RRCAT



Fig. 4. Sample Vane Fabricated at M/s. IGTR, Ahmedabad



Fig. 5. RRCAT Chemical facility lab personnel with plated chamber

### 2.2.4 Fabrication of First DTL Cavity and Development of Prototype Cavity

J. Zacharias, B P Ajith Kumar, R Mehta & R V Hariwal

The High Current Injector (HCI) project at Inter University Accelerator Centre uses a Radio Frequency Quadrupole (RFQ), Drift Tube Linac (DTL) and low beta superconducting cavities to accelerate heavy ions having  $A/q \leq 6$ , from the high temperature superconducting electron cyclotron resonance ion source (HTS-ECRIS called PKDELIS) to the existing superconducting linear accelerator (SC LINAC). The required output energy of the DTL is decided by the minimum input velocity ( $\beta = 0.06$ ) required for the existing superconducting LINAC. The beam dynamics and generation of the drift tube geometry is done using the LANA code [1]. A full scale prototype resonator has been fabricated [2] for validating the design. Frequency, voltage profile measurements and high power RF test have been done on a full size prototype resonator.

#### Fabrication of First DTL Cavity

The fabrication, copper plating and vacuum leak testing of first DTL tank was done at M/s Kaltech, Canada. Fabrication of ridges, stems and cooling channels started at Don Bosco Technical Institute in December 2012. Details of fabrication process is listed below

Ridges and stems were pre-machined with copper. Final machining was carried out to ensure required tolerances and sizes. As the required dimensional accuracy is  $\leq 50\mu\text{m}$ , stringent quality assurance checks were put in place at various stages of machining. For machining various high precision CNC machines, EDM, wire cutting machine and CMM were used.

Cooling channels and water sumps were provided on tanks, end plates, stems, ridges and flange collars. Innovative cooling mechanism was adopted for the ridges with extra volume for water circulation on ridge external surface. All channels were tested at 2 bar inlet water pressure.

Both top & bottom Ridges were mounted and stem mounting faces were aligned within required accuracy and parallelism within two faces were obtained by machining and was measured using CMM. Stems were mounted and aligned for needed gap lengths. High precision machined rods of 50 micron less diameter than the ID of the stems was used for final alignment.

After complete assembly cavity was tested for vacuum leak test. System was leak tested upto  $5 \times 10^{-8}$  mbar l/sec leak rate.

#### Frequency and Q Measurement

Frequency and Quality factor of cavity was measured in vacuum. Results are listed as below:

Frequency	:	98.95 MHz
Intrinsic Quality Factor	:	10400

As the frequency is higher than the designed value of 97.00 MHz, it will be brought to design value by trimming the ridges. The required trimming has been optimized by using CST program. Currently we are working on carrying out high power test on this cavity.

#### Prototype DTL Cavity Development

Meanwhile we had problem with the copper plating of prototype cavity. This cavity has been copper plated at RRCAT, Indore. We are in process of making end flanges for this cavity. These will be made out of 25 mm thick copper sheet. We plan to take up this cavity after high power test of first DTL cavity.

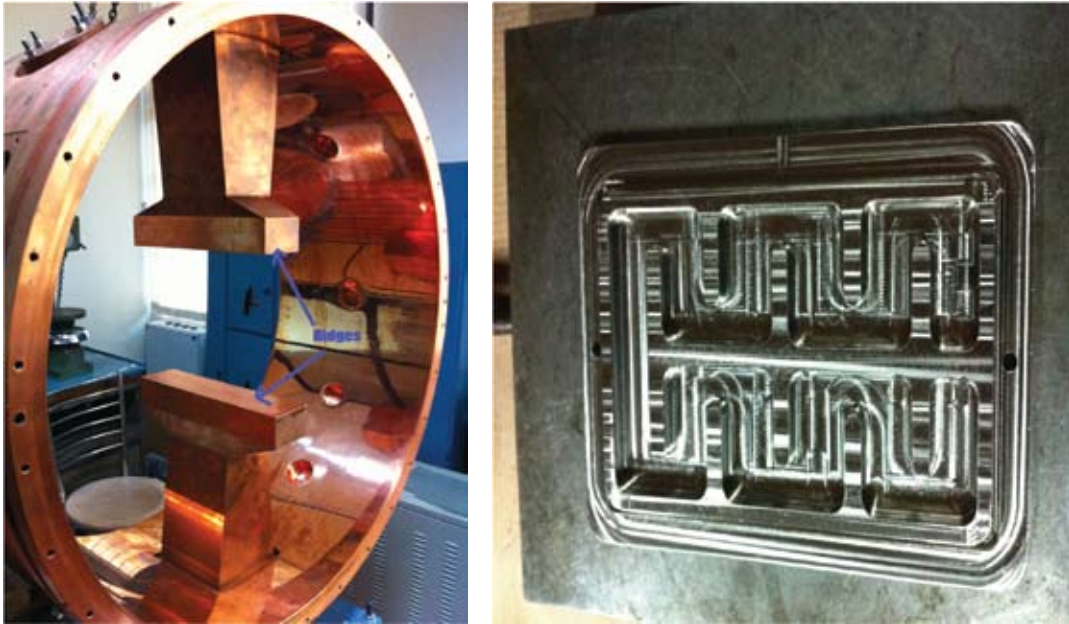


Fig. 1. Ridge Alignment and water cooling channels for end plates

#### References:

- [1] "Beam Optics and Resonator Design for the 97 MHz DTL at IUAC", Indian Particle Accelerator Conference - 2009, RRCAT, Indore, India.
- [2] "Mechanical Design, Fabrication and Initial Tests on Prototype Drift Tube Linac at IUAC", by J Zacharias, R Mehta, Ajith kumar B P and R V Hariwal, Indian Particle Accelerator Conference - 2011, InPAC2011, IUAC, New Delhi, India

### 2.2.5 Beam Transport System for HCI

Sarvesh Kumar, A Mandal

This year the major thrust has been given for finalization of beam transport system of HCI and development of controller for Multi Harmonic buncher. Beam transport elements viz. air cooled quadrupole magnets and beam diagnostic elements such as fast faraday cups etc are being developed for HCI. Power supplies for different magnets have been indigenously developed. Details of development activities are summarized below.

#### 2.2.5.1 Beam Optics of High Current Injector

Sarvesh Kumar, A Mandal

The beam optics of high current injector has been finalized after discussing with the committee formed by the director for this purpose. Special effort was given to match the input parameters of the RFQ and DTL. Simulations for the three sections LEBT, MEBT and HEBT have been carried out using codes TRANSPORT, GICOSY and TRACE3D.

The transverse and longitudinal beam optics of LEBT and MEBT section has been finalized using code TRANSPORT and TRACE3D. Then the initial beam parameters as well as beam tuning parameters throughout the transport section from these codes are converted to TRACK code input to provide final checking in terms of multiparticle beam dynamics simulations. The longitudinal bunching is provided by multi harmonic buncher, RFQ and a spiral buncher respectively. The beam dynamics using multiparticle simulation code for LEBT + MEBT section is shown in fig. 1a. It is clear from the TRACK output shown in fig. 1b that the energy spread of the beam keeps on increasing while reducing the time width of the bunch as the beam traverses from HTS-ECRIS to DTL.



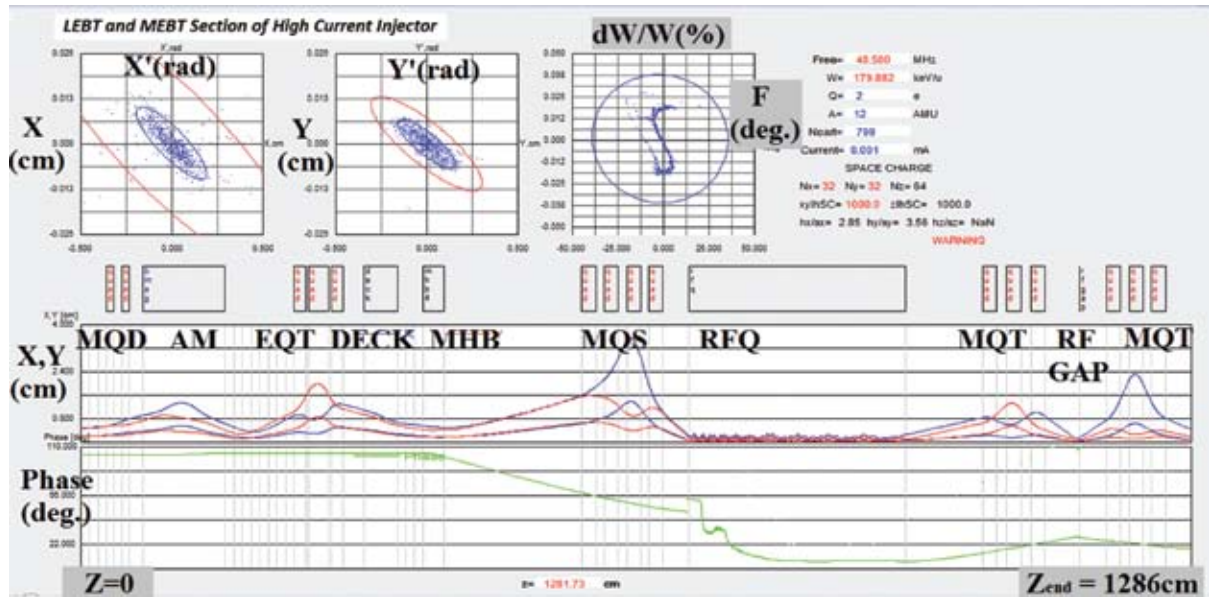


Fig. 1a. Beam dynamics simulations of LEBT and MEBT using TRACK code

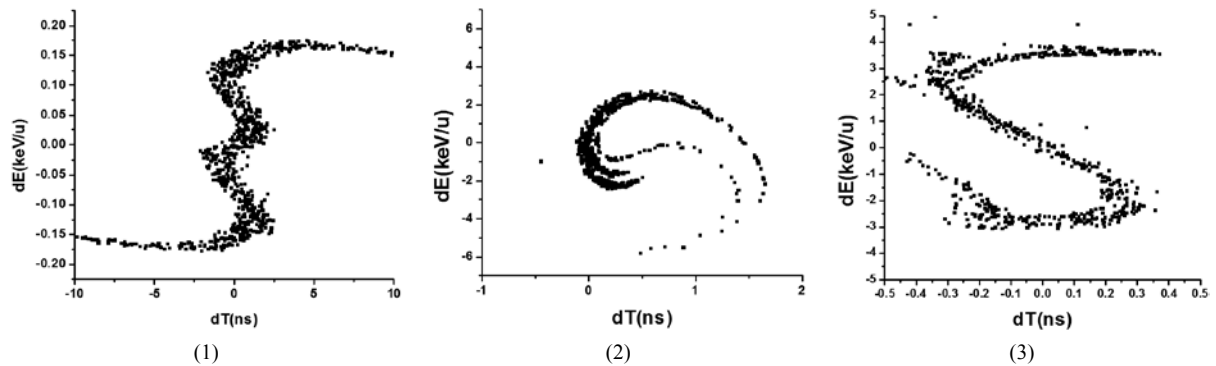


Fig. 1b. Longitudinal emittance plots at the entrance (1), exit of RFQ (2) and at the entrance of DTL (3) respectively by TRACK code

## II. High energy beam transport section (HEBT):

The beam coming out of DTL has to be transported to SC-LINAC through a long HEBT section which consists of four achromatic 90 deg. bends. The three bends are of similar type but the last one is different due to space constraint of accommodation of existing Mat. Sc. Beam line of Pelletron. Details of these achromats have been reported earlier. Now we have looked into higher order effects due to radii of curvature of entrance and exit field boundary (EFB) and fringe field effects of the quadrupoles. It is observed that EFB radius  $>2m$  of bending magnets has non-appreciable effect on the achromatic properties. The same achromat configuration can be used in energy dispersive mode by switching off the middle quadrupole Q4. This provides energy dispersion of  $2.6 \text{ cm}/\%dp/p$  corresponding to energy resolution 0.2%.

The configuration of both type of achromats in bending plane is shown in fig. 1c.

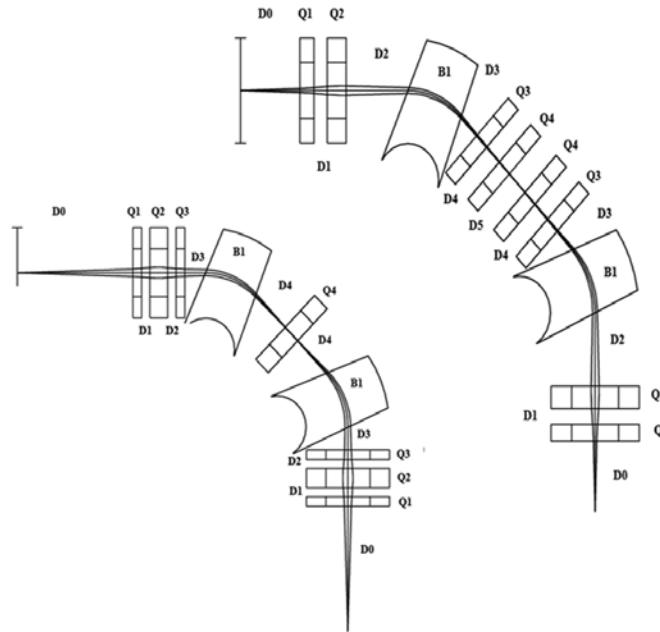


Fig. 1c. Configuration of Ist and IInd type of Achromat

### 2.2.5.2 Fabrication of Magnetic quadrupoles for LEBT section of HCI

Sarvesh Kumar, S.K.Saini, A.Mandal

The magnetic quadrupoles required before RFQ have been designed. The coil layout is shown in fig. 2b. Vector field opera codes have been used to optimize the shape of the pole profile longitudinally and Poisson code have been used to reduce the higher order harmonic contents by proper chamfering of the poles in transverse direction as shown in fig. 2c. The specifications of the coils are in Table-1. Coil diameter has been chosen in such a way to keep current density for ambient air cooling. Thirty numbers of coils have been fabricated by the local vendor. The fabrication of yoke and poles of the quadrupole is in process.

**Table-1: Coil Specifications**

Parameters	Before RFQ (Quartet)
Maximum Field (G)	1500
Ampere Turns (NI)	2331
Length of iron yoke(mm)	121
Pole Tip radius (mm)	44
SWG No. and dia. of coil (mm)	12, 2.64
Voltage ,current , Power required	16V, 6A, 96W
Chamfer Angles (deg.) (Longitudinal and Transverse)	21, 30



Fig. 2b: Air cooled coil Windings

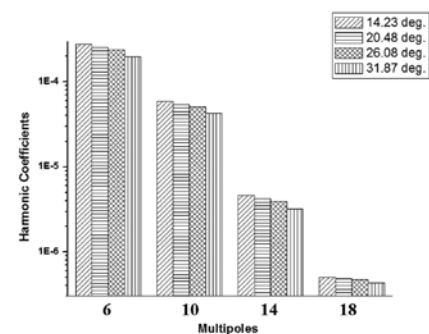


Fig. 2c: Harmonic Analysis

### 2.2.5.3 Development of magnet power supplies for HCI

S.K.Suman, Rajesh Kumar, Mukesh Kumar, A.Mandal

Program has been taken up to develop power supplies for air cooled quadrupoles and steerers. A linear current regulated power supply of 300 Watt has been ingeniously developed. It has been tested with

actual load and stability of power supply measured ~ 100PPM. The details of power supply is described in section 3.1.2.1.

## 2.3 CRYOGENICS

T.S.Datta, J.Chacko, A .Choudhury, J. Antony, M. Kumar, S. Babu, S.Kar, D.S. Mathuria , R.N.Dutt, R.G. Sharma and A.Roy

In this academic year, first time Linac beam tests were performed with all five beam line cryomodules together. In total 23 cavities, distributed in five cryomodules were cooled down to 4.2 K by using new Linde 750 W refrigerator and additional section of liquid helium distribution line. Prior to the long linac run (more than 100 days), performance test of new refrigerator, the modified cooling system with new distribution line and Complete Automation of Distribution System (CADS) were carried out successfully. The performance of beam acceleration tests is reported in Linac section.

### 2.3.1 Cryogenic Facility

#### I. Liquid Helium Plant

In this academic year both helium plants were operated for off-line testing of the niobium resonators in LINAC-II and III cryomodules and the beam acceleration through the LINAC. The total helium production was approximately 10,80,000 litres. Fig.1 shows the yearly LHe production. The fig.1 shows major enhancement of helium production which is mainly due to the three- months uninterrupted operation of new helium refrigerator for Linac run.

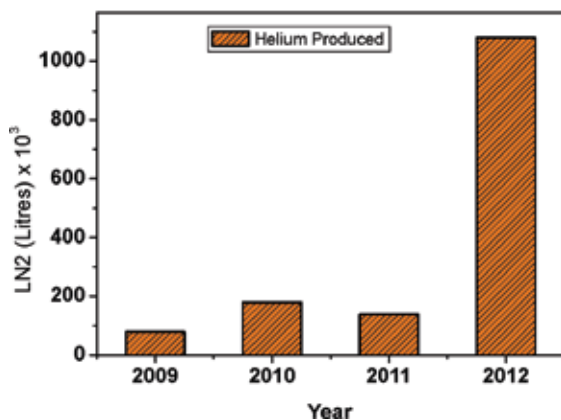


Fig.1. Yearly LHe Production

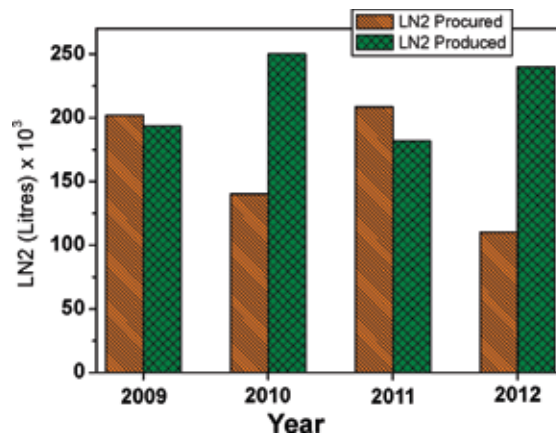


Fig. 2. Yearly LN2 Inventory

#### II. Liquid Nitrogen Plant

In this academic year, total in-house production of LN2 was 2,40,000 litres. LN2 procured from outside vendor was 1,10,000 L. Fig.2 shows the yearly LN2 production and amount of procurement. Liquid nitrogen consumption is reduced because of Linac run with the new helium refrigerator without liquid nitrogen precooling. During the beam acceleration through the LINAC, the new helium refrigerator was able to manage the static and dynamic heat load at 4.2K for all five cryostats without LN2 precooling. .

### 2.3.2 LINAC Cryomodules

In this academic year, for the first time, beam was accelerated through all the three accelerating cryomodules in the LINAC. The beam-line cryostats are cooled in combination of series or parallel flow scheme

using the new helium refrigerator. The cool-down of the LINAC was started with the parallel cooling of LINAC-I cryomodule and rebuncher cryostat. Then other cryomodules were cooled one after another. The complete cool down of Linac is shown in figure 3.

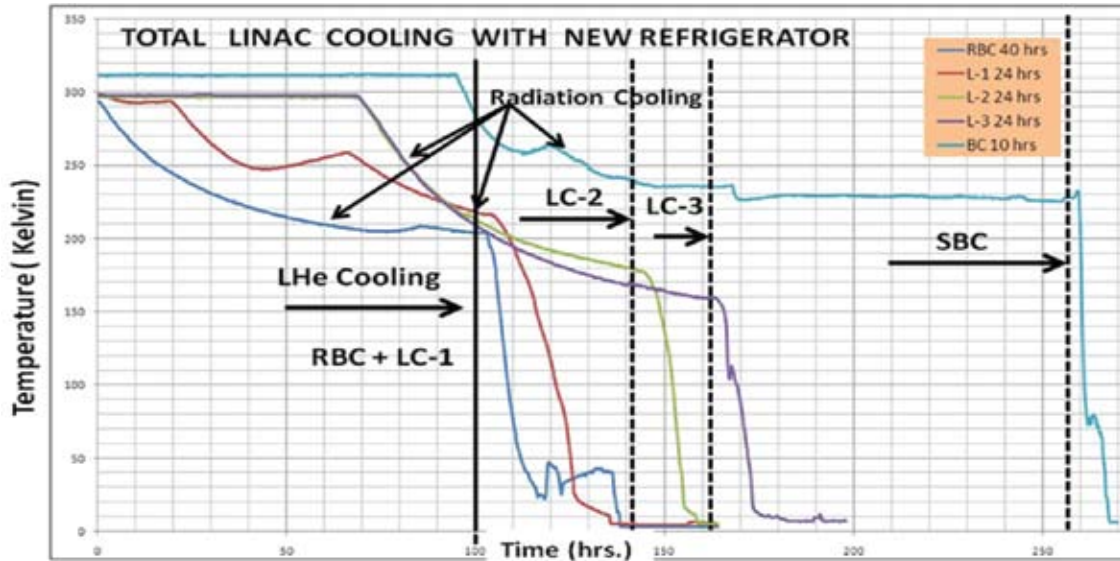


Fig. 3. Cooling sequences of five cryomodules with the new refrigerator

In this new scheme of cooling, the return cold gas could be fed to the three different thermodynamic point of the return flow (low pressure) of the refrigerator as shown in figure 4.

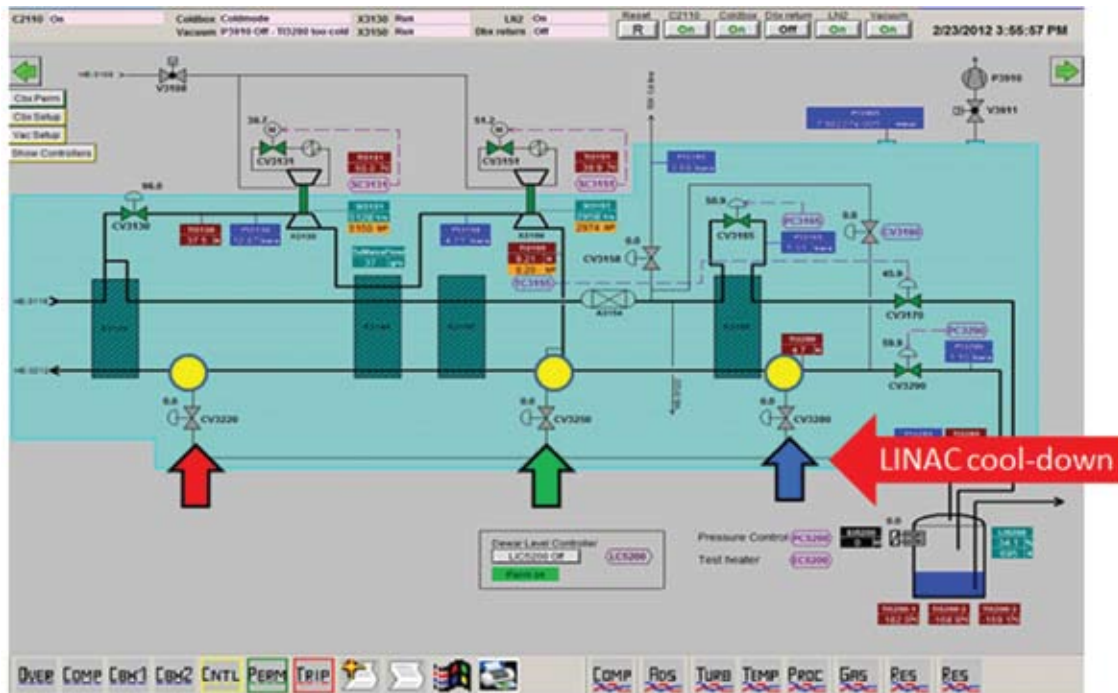


Fig. 4. Sample picture of cold box running parameters with return gas from Linac

The average cool-down rate of the resonators in LINAC-II and III with the additional header improved significantly and was 35 K/hr as against earlier of max 20 K/hr in the temperature range of 150K to 80 K and shown in figure 5. Second advantage of this new cooling scheme is better stability of helium vessel gas pressure as shown in figure 6.

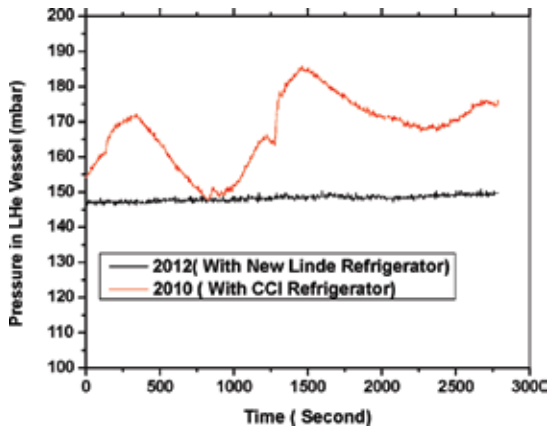


Fig. 5. Cool down profile in LC- II & LC-III

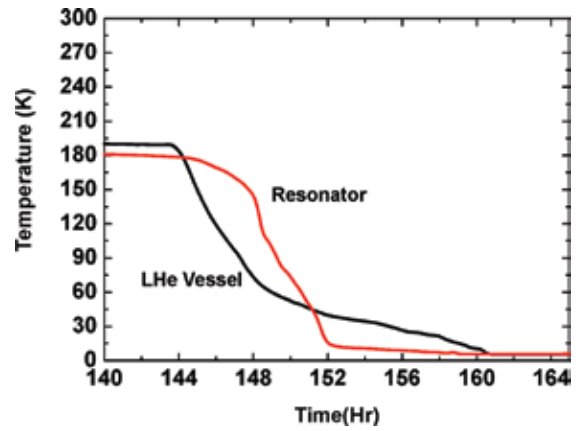


Fig. 6. Pressure fluctuation with new & old refrigerator

In this academic year , the cryogenic distribution system was operated by using newly developed control system (CADS). The schematic of the control page is given in the Fig. 7. The detailed performance analysis of cooling is under progress and will be reported in next year.

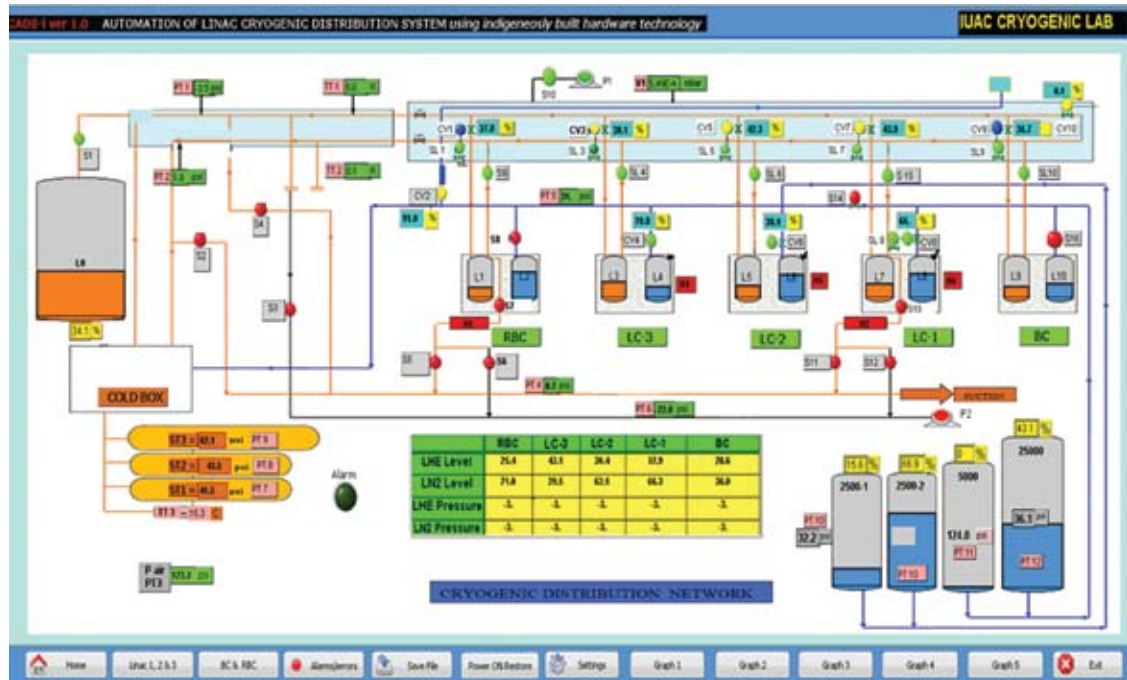


Fig. 7. The schematic of the CADS control system .